

Target prediction and a statistical sampling algorithm for RNA-RNA interaction

Fenix W.D. Huang¹, Jing Qin¹, Christian M. Reidys^{1,2*}, and Peter F. Stadler^{3–7}

¹Center for Combinatorics, LPMC-TJKLC, Nankai University Tianjin 300071, P.R. China

²College of Life Science, Nankai University Tianjin 300071, P.R. China

³Bioinformatics Group, Department of Computer Science, and Interdisciplinary Center for Bioinformatics, University of Leipzig, Härtelstrasse 16-18, D-04107 Leipzig, Germany.

⁴Max Planck Institute for Mathematics in the Sciences, Inselstrasse 22, D-04103 Leipzig, Germany

⁵RNomics Group, Fraunhofer Institut for Cell Therapy and Immunology, Perlickstraße 1, D-04103 Leipzig, Germany

⁶Inst. f. Theoretical Chemistry, University of Vienna, Währingerstrasse 17, A-1090 Vienna, Austria

⁷The Santa Fe Institute, 1399 Hyde Park Rd., Santa Fe, New Mexico, USA

Received on *****; revised on *****; accepted on *****

Associate Editor: *****

ABSTRACT

It has been proven that the accessibility of the target sites has a critical influence for miRNA and siRNA. In this paper, we present a program, `rip2.0`, not only the energetically most favorable targets site based on the hybrid-probability, but also a statistical sampling structure to illustrate the statistical characterization and representation of the Boltzmann ensemble of RNA-RNA interaction structures. The outputs are retrieved via backtracing an improved dynamic programming solution for the partition function based on the approach of Huang *et al.* (Bioinformatics). The $O(N^6)$ time and $O(N^4)$ space algorithm is implemented in C (available from <http://www.combinatorics.cn/cbpc/rip2.html>).

1 INTRODUCTION

Noncoding RNAs have been found to have roles in a great variety of processes, including transcriptional regulation, chromosome replication, RNA processing and modification, messenger RNA stability and translation, and even protein degradation and translocation. Direct base-pairing with target RNA or DNA molecules is central to the function of some ncRNAs (Storz, 2002). Examples include the regulation of translation in both prokaryotes (Narberhaus and Vogel, 2007) and eukaryotes (McManus and Sharp, 2002; Banerjee and Slack, 2002), the targeting of chemical modifications (Bachelier *et al.*, 2002), as well as insertion editing (Benne, 1992), transcriptional control (Kugel and Goodrich, 2007). The common theme in many RNA classes, including miRNAs, siRNAs, snRNAs, gRNAs, and snoRNAs is the formation of RNA-RNA interaction structures that are more complex than simple sense-antisense interactions.

The hybridization energy is a widely used criterion to predict RNA-RNA interactions (Rehmsmeier *et al.*, 2004; Tjaden *et al.*, 2006; Busch *et al.*, 2008). It has been proven that the accessibility of the target sites has a critical influence for miRNA and siRNA (Ameres and Schroeder, 2007; Kertesz *et al.*, 2007; Kretschmer-Kazemi Far and Sczakiel, 2003). Although a lot regulatory ncRNAs has already been identified, the number of experimentally verified target sites is much smaller, which stimulate a great demand to restrain the list of putative targets. In its most general form, the RNA-RNA interaction problem (RIP) is NP-complete (Alkan *et al.*, 2006; Mneimneh, 2007). The argument for this statement is based on an extension of the work of Akutsu (2000) for RNA folding with pseudoknots. Polynomial-time algorithms can be derived, however, by restricting the space of allowed configurations in ways that are similar to pseudoknot folding algorithms (Rivas and Eddy, 1999). The second major problem concerns the energy parameters since the standard loop types (hairpins, internal and multiloops) are insufficient; for the additional types, such as kissing hairpins, experimental data are virtually absent. Tertiary interactions, furthermore, are likely to have a significant impact.

Several circumscribed approaches of target prediction have been considered in the literature. The simplest approach concatenates the two interacting sequences and subsequently employs a slightly modified standard secondary structure folding algorithm. For instance, the algorithms `RNAcofold` (Hofacker *et al.*, 1994; Bernhart *et al.*, 2006), `pairfold` (Andronescu *et al.*, 2005), and `NUPACK` (Ren *et al.*, 2005) subscribe to this strategy. The main problem of this approach is that it cannot predict important motifs such as kissing-hairpin loops. The paradigm of concatenation has also been generalized to the pseudoknot folding algorithm of Rivas and Eddy (1999). The resulting model, however, still does not generate all relevant interaction structures (Chitsaz *et al.*, 2009; Qin and Reidys, 2008). An alternative line of thought is to neglect

*to whom correspondence should be addressed. Phone: *86-22-2350-6800; Fax: *86-22-2350-9272; duck@santafe.edu

all internal base-pairings in either strand and to compute the minimum free energy (mfe) secondary structure for their hybridization under this constraint. For instance, RNAplex and RNAhybrid (Rehmsmeier *et al.*, 2004) follows this line of thought. RNAup (Mückstein *et al.*, 2006, 2008) and intaRNA (Busch *et al.*, 2008) restrict interactions to a single interval that remains unpaired in the secondary structure for each partner. Due to the highly conserved interaction motif, snoRNA/target complexes are treated more efficiently using a specialized tool (Tafer *et al.*, 2009) however. Pervouchine (2004) and Alkan *et al.* (2006) independently derived and implemented minimum free energy (mfe) folding algorithms for predicting the joint secondary structure of two interacting RNA molecules with polynomial time complexity. In their model, a “joint structure” means that the intramolecular structures of each molecule are pseudoknot-free, the intermolecular binding pairs are noncrossing and there exist no so-called “zig-zags”. The optimal “joint structure” can be computed in $O(N^6)$ time and $O(N^4)$ space by means of dynamic programming.

Recently, Chitsaz *et al.* (2009) and Huang *et al.* (2009) independently presented piRNA and rip1.0, tools that use dynamic programming algorithm to compute the partition function of “joint structures”, both in $O(N^6)$ time. Albeit differing in design details, they are equivalent. In addition, Huang *et al.* (2009) identified in rip1.0 a basic data structure that forms the basis for computing additional important quantities such as the base pairing probability matrix. However, since the probabilities of hybrid is not simply a sum of the probabilities of the exterior arcs which are not independent, rip1.0 can not solve the probability of a hybrid.

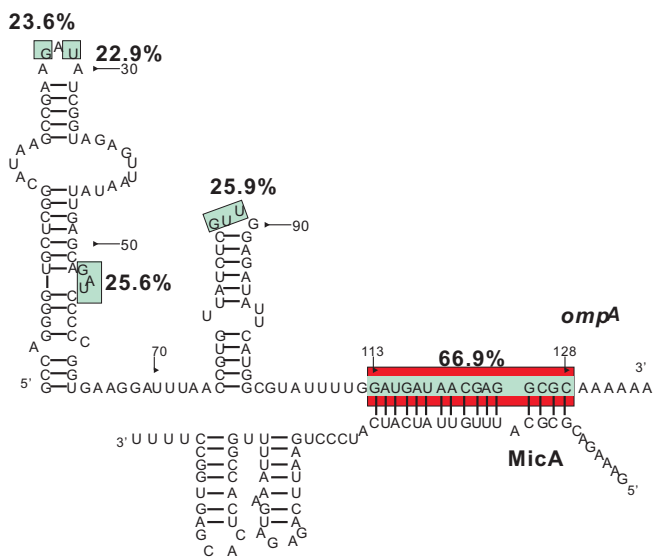


Fig. 1. The natural structure of *ompA-MicA* (Udekwu *et al.*, 2005), in which the target site are colored in red and the regions colored in green are the ones with the first five region-probabilities. The target sites $R[i, j]$ of *ompA* (interacts with *MicA*) whose probabilities larger than 10^{-1} are showed in Tab. 3.1.

The calculation of equilibrium partition functions and base-pairing probabilities is an important advance toward the characterization of the Boltzmann ensemble of RNA-RNA interaction

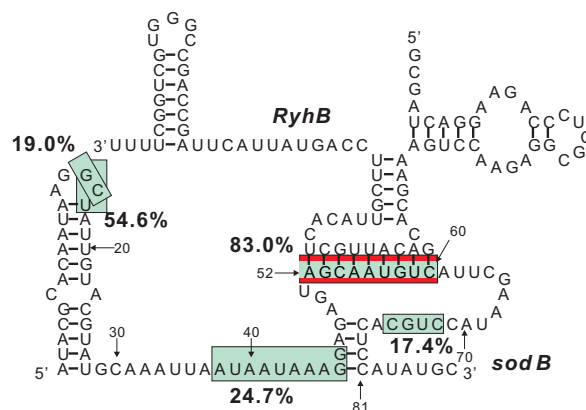


Fig. 2. The natural structure of *sodB-RyhB* (Geissmann and Touati, 2004), in which the target site are colored in red and the regions colored in green are the ones with the first five region-probabilities. The target sites $R[i, j]$ of *sodB* (interacts with *RyhB*) whose probabilities larger than 10^{-1} are showed in Tab. 3.1.

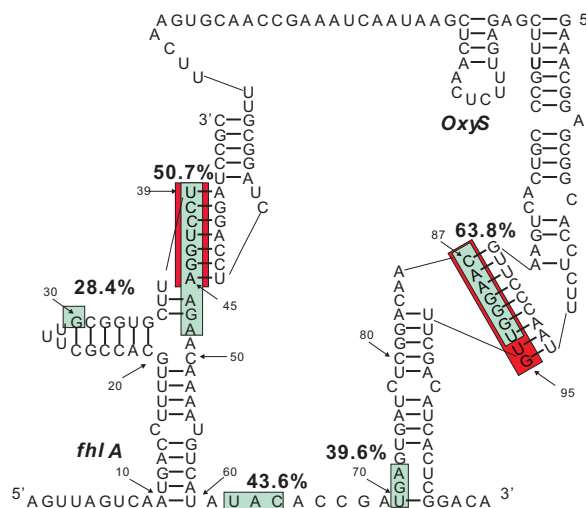


Fig. 3. The natural structure of *fhIA-OxyS* (Chitsaz *et al.*, 2009), in which the target site are colored in red and the regions colored in green are the ones with the first five region-probabilities. The target sites $R[i, j]$ of *fhIA* (interacts with *OxyS*) whose probabilities larger than 10^{-1} are showed in Tab. 3.1.

structures. However, this elegant algorithm does not generate any structures. However, as Ding and Lawrence (2003) suggested with prototype algorithms, the generation of a statistically representative sample of secondary structures may provide a resolution to this dilemma.

In contrast to rip1.0, given two RNA sequences, the output of rip2.0 consists of not only the partition function, the base pairing probability matrix, but also the contact-region probability matrix based on the hybrid probabilities via introducing a new component “hybrid” in the decomposition process and a statistically sampled RNA-RNA structure based on the probability-matrices. At the same time, we decrease the storage space from 4D-matrices and 2D-matrices to 4D-matrices and 2D-matrices.

2 PARTITION FUNCTION

2.1 Background

Let us first review some basic concepts has been introduced by Huang *et al.* (2009), see supplement material (SM) for a full-version.

Given two RNA sequences R and S (e.g. an antisense RNA and its target) with N and M vertices, we index the vertices such that R_1 is the 5' end of R and S_1 denotes the 3' end of S . The edges of R and S represent the intramolecular base pairs. A *joint structure*, $J(R, S, I)$, is a graph with the following properties, see Fig. 4, (B):

1. R, S are secondary structures (each nucleotide being paired with at most one other nucleotide via hydrogen bonds, without internal pseudoknots);
2. I is a set of arcs of the form $R_i S_j$ without pseudoknots, i.e., if $R_{i_1} S_{j_1}, R_{i_2} S_{j_2} \in I$ where $i_1 < i_2$, then $j_1 < j_2$ holds;
3. There are no zig-zags, see Fig. 4, (A).

Joint structures are exactly the configurations that are considered in the maximum matching approach of Pervouchine (2004), in the energy minimization algorithm of Alkan *et al.* (2006), and in the partition function approach of Chitsaz *et al.* (2009). The subgraph of a joint structure $J(R, S, I)$ induced by a pair of subsequences $\{R_i, R_{i+1}, \dots, R_j\}$ and $\{S_h, S_{h+1}, \dots, S_\ell\}$ is denoted by $J_{i,j;h,\ell}$. In particular, $J(R, S, I) = J_{1,N;1,M}$. We say $R_a R_b (S_a S_b, R_a S_b) \in J_{i,j;h,\ell}$ if and only if $R_a R_b (S_a S_b, R_a S_b)$ is an edge of the graph $J_{i,j;h,\ell}$. Furthermore, $J_{i,j;h,\ell} \subset J_{a,b;c,d}$ if and only if $J_{i,j;h,\ell}$ is a subgraph of $J_{a,b;c,d}$ induced by $\{R_i, \dots, R_j\}$ and $\{S_h, \dots, S_\ell\}$. Given a joint structure, $J_{a,b;c,d}$, its tight structure (ts)

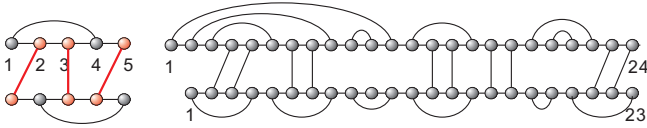


Fig. 4. (A): A zigzag, generated by $R_2 S_1, R_3 S_3$ and $R_5 S_4$ (red). (B): the joint structure $J_{1,24;1,23}$, we color the different segments and tight structures in which $J_{1,24;1,23}$ decomposes.

$J_{a',b';c',d'}$ is either a single exterior arc $R_{a'} S_{c'}$ (in the case $a' = b'$ and $c' = d'$), or the minimal block centered around the leftmost and rightmost exterior arcs α_l, α_r , (possibly being equal) and an interior arc subsuming both, i.e., $J_{a',b';c',d'}$ is tight in $J_{a,b;c,d}$ if it has either an arc $R_{a'} R_{b'}$ or $S_{c'} S_{d'}$ if $a' \neq b'$ or $c' \neq d'$.

In the following, a ts is denoted by $J_{i,j;h,\ell}^T$. If $J_{a',b';c',d'}$ is tight in $J_{a,b;c,d}$, then we call $J_{a,b;c,d}$ its envelope. There are only four basic types of ts, see Fig. 5:

$$\circ : \{R_i S_h\} = J_{i,j;h,\ell}^\circ \text{ and } i = j, h = \ell;$$

$$\nabla : R_i R_j \in J_{i,j;h,\ell}^\nabla \text{ and } S_h S_\ell \notin J_{i,j;h,\ell}^\nabla;$$

$$\square : \{R_i R_j, S_h S_\ell\} \in J_{i,j;h,\ell}^\square;$$

$$\triangle : S_h S_\ell \in J_{i,j;h,\ell}^\triangle \text{ and } R_i R_j \notin J_{i,j;h,\ell}^\triangle.$$

2.2 Refined decomposition grammar for target prediction

The unique ts decomposition would in principle already suffice to construct a partition function algorithm. Indeed, each decomposition step corresponds

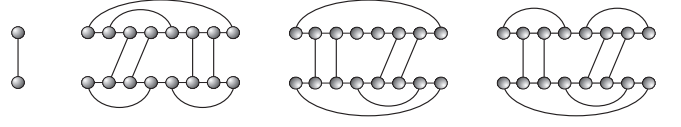


Fig. 5. From left to right: tights of type \circ, ∇, \square and \triangle .

to a multiplicative recursion relation for the partition functions associated with the joint structures. From a practical point of view, however, this would result in an unwieldy expensive implementation. The reason are the multiple break points a, b, c, d, \dots , each of which correspond to a nested for -loop.

We therefore need a refined decomposition that reduced the number of break points. To this end we call a joint structure *right-tight* (rts), $J_{i_1,j_1;r_1,s_1}^{RT}$ in $J_{i_1,j_1;r_1,s_1}$ if its rightmost block is a $J_{i_1,j_1;r_1,s_1}$ -ts and *double-tight* (dts), $J_{i_1,j_1;r_1,s_1}^{DT}$ in $J_{i_1,j_1;r_1,s_1}$ if both of its left- and rightmost blocks are $J_{i_1,j_1;r_1,s_1}$ -ts's. In particular, for the convenient of the computation, we assume the single interaction arc as a special case of dts, i.e. $J_{i_1,i_1;r_1,r_1}^{DT} = R_{i_1} S_{r_1}$. In order to obtain the probability of a hybrid $J_{i_1,i_\ell;j_1,j_\ell}^{\text{Hy}}$ via the backtracing method used in (Huang *et al.*, 2009), we introduce the hybrid structure, $J_{i_1,i_\ell;j_1,j_\ell}^{\text{Hy}}$, as a new block item used in the decomposition process. We adopt the point of view of Algebraic Dynamic Programming (Giegerich and Meyer, 2002) and regard each decomposition rule as a production in a suitable grammar. Fig. 6 summarizes three major steps in the decomposition: (I) "interior arc-removal" to reduce ts. The scheme is complemented by the usual loop decomposition of secondary structures, and (II) "block-decomposition" to split a joint structure into two blocks.

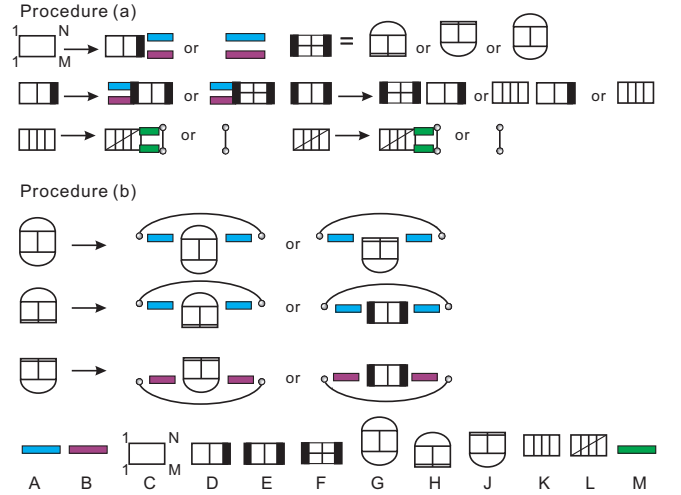


Fig. 6. Illustration of Procedure (a) the reduction of arbitrary joint structures and right-tight structures, and Procedure (b) the decomposition of tight structures. The panel below indicates the 10 different types of structural components: **A, B**: maximal secondary structure segments $R[i, j], S[r, s]$; **C**: arbitrary joint structure $J_{1,N;1,M}$; **D**: right-tight structures $J_{i,j;r,s}^{RT}$; **E**: double-tight structure $J_{i,j;r,s}^{DT}$; **F** tight structure of type ∇, \triangle or \square ; **G**: type \square tight structure $J_{i,j;r,s}^\square$; **H**: type ∇ tight structure $J_{i,j;r,s}^\nabla$; **J**: type \triangle tight structure $J_{i,j;r,s}^\triangle$; **K**: hybrid structure $J_{i,j;h,\ell}^{\text{Hy}}$; **L**: substructure of a hybrid $J_{i,j;h,\ell}^{\text{Hy}}$ such that $R_i S_\ell$ and $R_h S_\ell$ are exterior arcs; **M**: isolated segment $R[i, j]$ or $S[h, \ell]$.

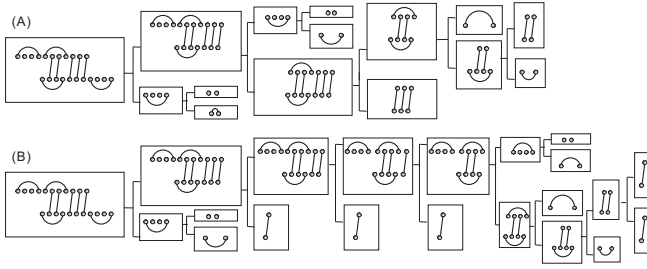


Fig. 7. The decomposition trees $T_{J_{1,15;1,8}}$ for the joint structure $J_{1,15;1,8}$ according to the grammar in `rip2.0` (A) and `rip1.0` (B), respectively.

According to the decomposition rule, a given joint structure decomposed into interior arcs and hybrids, see Figure 7 (A). The details of the decomposition procedures are collected in SM, Section 2, where we show that for each joint structure $J_{1,N;1,M}$ we indeed obtain a unique decomposition-tree (parse-tree), denoted by $T_{J_{1,N;1,M}}$. More precisely, $T_{J_{1,N;1,M}}$ has root $J_{1,N;1,M}$ and all other vertices correspond to a specific substructure of $J_{1,N;1,M}$ obtained by the successive application of the decomposition steps of Fig. 6 and the loop decomposition of the secondary structures. The decomposition trees of a concrete example generated according to `rip2.0` and `rip1.0` is shown in Fig. 7 (A) and (B), respectively.

Let us now have a closer look at the energy evaluation of $J_{i,j;h,\ell}$. Each decomposition step in Fig. 6 results in substructures whose energies we assume to contribute additively and generalized loops that need to be evaluated directly. There are the following two scenarios:

I. Interior Arc removal. The first type of decomposition is focus on decomposing ts which is similar as the approach deduced by Huang *et al.* (2009). Most of the decomposition operations in Procedure (b) displayed in Fig. 6 can be viewed as the “removal” of an arc (corresponding to the closing pair of a loop in secondary structure folding) followed by a decomposition. Both: the loop-type and the subsequent possible decomposition steps depend on the newly exposed structural elements. W.l.o.g., we may assume that we open an interior base pair $R_i R_j$.

For instance, a rts $J_{p,q,r,s}^{RT}$ (denoted by “D” in Fig. 6) we need to determine the type of the exposed pairs of both $R[p,q]$ and $S[r,s]$. Hence each such structure will be indexed by two types lies in $\{E, M, K, F\}$. Analogously, there are in total four types of a hybrid $J_{i,j;h,\ell}^{Hy}$, i.e. $\{J_{i,j;h,\ell}^{Hy,EE}, J_{i,j;h,\ell}^{Hy,EK}, J_{i,j;h,\ell}^{Hy,KE}, J_{i,j;h,\ell}^{Hy,KK}\}$.

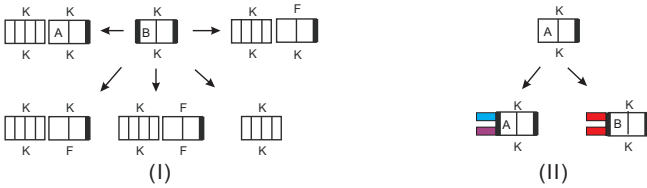


Fig. 8. (I) Decomposition of $J_{i,j;h,\ell}^{RT,MK}$ and (II) decomposition of $J_{i,j;h,\ell}^{DT,KKB}$.

II. Block decomposition. The second type of decomposition is the splitting of joint structures into “blocks”. There are two major differences in contrast to the method used in Huang *et al.* (2009). First, we introduce the hybrid itself as a new block item in the grammar and furthermore decompose a hybrid via simultaneously removing a single exterior arc. Second, we split the whole interaction structure into blocks via the alternating decompositions of a rts and a dts as showed in the Procedure (a) of Fig. 6.

In order to make sure the maximality of a hybrid, the rts’s $J_{i,j;h,\ell}^{RT,KK}$, $J_{i,j;h,\ell}^{RT,KE}$, $J_{i,j;h,\ell}^{RT,EK}$ and $J_{i,j;h,\ell}^{RT,EE}$ may appear in two ways, depending on whether or not there exists an exterior arc $R_{i_1} S_{j_1}$ such that $R[i, i_1 - 1]$ and $S[j, j_1 - 1]$ are isolated segments. If there exists, we say rts is of type (B) or (A), otherwise. Similarly, a dts, $J_{i,j;h,\ell}^{DT,KK}$, $J_{i,j;h,\ell}^{DT,KE}$, $J_{i,j;h,\ell}^{DT,EK}$ or $J_{i,j;h,\ell}^{DT,EE}$ is of type (B) or (A) depending on whether $R_i S_h$ is an exterior arc. For instance, Fig. 8 (I) displays the decomposition of $J_{i,j;h,\ell}^{DT,KKB}$ into hybrid and rts with type (A) and furthermore Fig. 8 (II) displays the decomposition of $J_{i,j;h,\ell}^{RT,KKA}$.

Suppose $J_{i,j;r,\ell}^{DT}$ is a dts contained in a kissing loop, that is we have either $E_{R[i,j]}^e \neq \emptyset$ or $E_{S[h,\ell]}^e \neq \emptyset$. W.l.o.g., we may assume $E_{R[i,j]}^e \neq \emptyset$. Then at least one of the two “blocks” contains the exterior arc belonging to $E_{R[i,j]}^e$ labeled by K and F, otherwise, see Fig. 8 (I).

2.3 Examples for partition function recursions

The computation of the partition function proceeds “from the inside to the outside”, see equs. (2.2). The recursions are initialized with the energies of individual external base pairs and empty secondary structures on subsequences of length up to four. In order to differentiate multi- and kissing-loop contributions, we introduce the partition functions $Q_{i,j}^m$ and $Q_{i,j}^k$. Here, $Q_{i,j}^m$ denotes the partition function of secondary structures on $R[i, j]$ or $S[i, j]$ having at least one arc contained in a multi-loop. Similarly, $Q_{i,j}^k$ denotes the partition function of secondary structures on $R[i, j]$ or $S[i, j]$ in which at least one arc is contained in a kissing loop. Let $J_{i,j;h,\ell}^{\xi, Y_1 Y_2 Y_3}$ be the set of substructures $J_{i,j;h,\ell} \subset J_{1,N;1,M}$ such that $J_{i,j;h,\ell}$ appears in $T_{J_{1,N;1,M}}$ as an interaction structure of type $\xi \in \{DT, RT, \nabla, \Delta, \square, \circ\}$ with loop-subtypes $Y_1, Y_2 \in \{M, K, F\}$ on the sub-intervals $R[i, j]$ and $S[h, \ell]$, $Y_3 \in \{A, B\}$. Let $Q_{i,j;h,\ell}^{\xi, Y_1 Y_2 Y_3}$ denote the partition function of $J_{i,j;h,\ell}^{\xi, Y_1 Y_2 Y_3}$.

For instance, the recursion for $Q_{i,j;h,\ell}^{DT,KKB}$ displayed in Figure 8 (I) is equivalent to:

$$\begin{aligned} Q_{i,j;h,\ell}^{RT,MK} &= \sum_{i_1, h_1} Q_{i, i_1; h, h_1}^{Hy, KK} Q_{i_1+1, j; h_1+1, \ell}^{RT, KKA} + Q_{i, i_1; h, h_1}^{Hy, KK} Q_{i_1+1, j; h_1+1, \ell}^{RT, KF} \\ &+ Q_{i, i_1; h, h_1}^{Hy, KK} Q_{i_1+1, j; h_1+1, \ell}^{RT, FF} + Q_{i, i_1; h, h_1}^{Hy, KK} Q_{i_1+1, j; h_1+1, \ell}^{RT, FK} + Q_{i, i_1; h, h_1}^{Hy, KK} \end{aligned} \quad (2.1)$$

In which, the recursions for $J_{i,j;h,\ell}^{Hy,EE}$, $J_{i,j;h,\ell}^{Hy,EK}$, $J_{i,j;h,\ell}^{Hy,KE}$, and $J_{i,j;h,\ell}^{Hy,KK}$ read:

$$\begin{aligned} Q_{i,j;h,\ell}^{Hy,EE} &= \sum_{i_1, h_1} Q_{i, i_1; h, h_1}^{Hy, EE} e^{-(\sigma + \sigma G_{i_1, h_1}^{Int})}; \\ Q_{i,j;h,\ell}^{Hy,EK} &= \sum_{i_1, h_1} Q_{i, i_1; h, h_1}^{Hy, EK} e^{-(\sigma + \sigma G_{i_1, h_1}^{Int} + (\ell - h_1 - 1)\beta_3)}; \\ Q_{i,j;h,\ell}^{Hy,KE} &= \sum_{i_1, h_1} Q_{i, i_1; h, h_1}^{Hy, KE} e^{-(\sigma + \sigma G_{i_1, h_1}^{Int} + (j - i_1 - 1)\beta_3)}; \\ Q_{i,j;h,\ell}^{Hy,KK} &= \sum_{i_1, h_1} Q_{i, i_1; h, h_1}^{Hy, KK} e^{-(\sigma + \sigma G_{i_1, h_1}^{Int} + (j + \ell - i_1 - h_1 - 2)\beta_3)}. \end{aligned} \quad (2.2)$$

3 BACKTRACING

3.1 target prediction

Given two RNA sequences, our sample space is the ensemble of all the possible joint interaction structures. Let Q^I denote the partition function which sums over all the possible joint structures. The probability measure of a given joint structure $J_{1,N;1,M}$ is given by

$$\mathbb{P}_{J_{1,N;1,M}} = \frac{Q_{J_{1,N;1,M}}}{Q^I}. \quad (3.1)$$

In contrast to the computation of the partition function “from the inside to the outside”, the computation of the substructure-probabilities are obtained “from the outside to the inside” via total probability formula (TPF). That is, the longest-range substructures are computed first. This is analogous to McCaskill’s algorithm for secondary structures (McCaskill, 1990).

Set $J = J_{1,N;1,M}$, $T = T_{J_{1,N;1,M}}$ and let $\Lambda_{J_{i,j;h,\ell}} = \{J | J_{i,j;h,\ell} \in T\}$ denote the set of all joint structures J such that $J_{i,j;h,\ell}$ is a vertex in the decomposition tree T . Then

$$\mathbb{P}_{J_{i,j;h,\ell}} = \sum_{J \in \Lambda_{J_{i,j;h,\ell}}} \mathbb{P}_J. \quad (3.2)$$

By virtue of TPF, set θ_s be the possible parent-structure of $J_{i,j;h,\ell}$ and $\mathbb{P}_{J_{i,j;h,\ell}|\theta_s}$ be the conditional probability, we have $\mathbb{P}_{J_{i,j;h,\ell}} = \sum_s \mathbb{P}_{J_{i,j;h,\ell}|\theta_s} \mathbb{P}_{\theta_s}$.

Let $\mathbb{P}_{i,j;h,\ell}^{\xi, Y_1 Y_2 Y_3}$ be the probability of $J_{i,j;h,\ell}^{\xi, Y_1 Y_2 Y_3}$. For instance, $\mathbb{P}_{i,j;h,\ell}^{RT, MKA}$ is the sum over all the probabilities of substructures $J_{i,j;h,\ell} \in T_{J_{1,N;1,M}}$ such that $J_{i,j;h,\ell} \in \mathbb{J}_{i,j;h,\ell}^{RT, MKA}$, i.e. a rts of type A and $R[i, j]$, $S[h, \ell]$ are respectively enclosed by a multi-loop and kissing loop. Given a component, $\mathbb{J}_{i,j;h,\ell}^{\xi, Y_1 Y_2 Y_3}$ (showed in Figure 6), we say another component $\mathbb{J}_{i,j;h,\ell}^{\xi, Y_1 Y_2 Y_3}$ is its *parent-component* if and only if as a substructure, $\mathbb{J}_{i,j;h,\ell}^{\xi, Y_1 Y_2 Y_3}$ could be a parent structure of $\mathbb{J}_{i,j;h,\ell}^{\xi, Y_1 Y_2 Y_3}$ in the decomposition tree. Accordingly, we say $\mathbb{J}_{i,j;h,\ell}^{\xi, Y_1 Y_2 Y_3}$ is the *child-component* of $\mathbb{J}_{i,j;h,\ell}^{\xi, Y_1 Y_2 Y_3}$. For instance, $\mathbb{J}_{i_1, j_1; h_1, \ell_1}^{RT, KKB}$ is one of the parent-component of $\mathbb{J}_{i,j;h,\ell}^{Hy, KKB}$, see Figure. 8 (I). Set Θ_s be one of the possible parent-component of $\mathbb{J}_{i,j;h,\ell}^{\xi, Y_1 Y_2 Y_3}$. Accordingly, we have

$$\mathbb{P}_{i,j;h,\ell}^{\xi, Y_1 Y_2 Y_3} = \sum_s \mathbb{P}_{i,j;h,\ell|\Theta_s}^{\xi, Y_1 Y_2 Y_3} \mathbb{P}_{\Theta_s}, \quad (3.3)$$

where by definition

$$\mathbb{P}_{i,j;h,\ell}^{\xi, Y_1 Y_2 Y_3} = \sum_{J_{i,j;h,\ell} \in \mathbb{J}_{i,j;h,\ell}^{\xi, Y_1 Y_2 Y_3}} \mathbb{P}_{J_{i,j;h,\ell}}. \quad (3.4)$$

Furthermore, in the programme, we calculate $\mathbb{P}_{i,j;h,\ell|\Theta_s}^{\xi, Y_1 Y_2 Y_3} \mathbb{P}_{\Theta_s}$ for all s during the decomposition of Θ_s . I.e. given \mathbb{P}_{Θ_s} , we have $\mathbb{P}_{\Theta_s} = \sum_i \mathbb{P}_{\epsilon_i|\Theta_s} \mathbb{P}_{\epsilon_i}$, where $\mathbb{P}_{\epsilon_i|\Theta_s}$ denotes the conditional probability of the event that given Θ_s is the parent-component, ϵ_i is its child-component. In particular, we have $\mathbb{P}_{i,j;h,\ell|\Theta_s}^{\xi, Y_1 Y_2 Y_3} = \mathbb{P}_{\epsilon_m|\Theta_s}$ for some m .

Since the four subclasses of $J_{i,j;h,\ell}^{Hy}$, i.e. $J_{i,j;h,\ell}^{Hy, EE}$, $J_{i,j;h,\ell}^{Hy, EK}$, $J_{i,j;h,\ell}^{Hy, KE}$ and $J_{i,j;h,\ell}^{Hy, KK}$ are independent, we obtain

$$\mathbb{P}_{i,j;h,\ell}^{Hy} = \mathbb{P}_{i,j;h,\ell}^{Hy, EE} + \mathbb{P}_{i,j;h,\ell}^{Hy, EK} + \mathbb{P}_{i,j;h,\ell}^{Hy, KE} + \mathbb{P}_{i,j;h,\ell}^{Hy, KK}. \quad (3.5)$$

Given a hybrid $J_{i,j;h,\ell}^{Hy}$, recall the definition target sites are $R[i, j]$ and $S[h, \ell]$. The probability of a target site $R[i, j]$ is defined by

$$\mathbb{P}_{R[i,j]}^{\text{tar}} = \sum_{h,\ell} \mathbb{P}_{i,j;h,\ell}^{Hy}. \quad (3.6)$$

Analogously, we define $\mathbb{P}_{R[i,j]}^{\text{tar}}$. We predict the optimal interaction region with maximal probability, i.e.

$$\mathbb{P}^{\text{opt}} = \max_{i,j} \mathbb{P}_{R[i,j]}^{\text{tar}}. \quad (3.7)$$

3.2 Statistically generating interaction structure

In this section, we generalize the idea of Ding and Lawrence (2003) in order to draw a representative sample from the Boltzmann equilibrium distribution of RNA interaction structures. The section is divided into two parts. At first we illustrate the correspondence between the decomposition grammar, i.e. the recursions for partition functions and the sampling probabilities for mutually exclusive cases and secondly, we describe the sampling algorithm.

The calculation of the sampling probabilities is based on the recurrences of the partition functions since for mutually exclusive and exhaustive cases,

113,128: 66.9%	87,89: 25.9%	53,55: 25.6%	27,27: 23.6%
29,29: 22.9%	39,40: 21.1%	27,28: 20.9%	67,69: 16.6%
115,128: 16.6%	36,41: 15.0%	36,40: 13.0%	26,28: 12.3%
67,70: 10.9%	55,56: 10.3%		

Table 1. The target sites $R[i, j]$ of *ompA* (interacts with *MicA*) whose probabilities larger than 10^{-1} .

52,60: 83.0%	15,17: 54.6%	38,47: 24.7%	15,16: 19.0%
72,75: 17.4%	77,78: 16.8%	45,47: 14.2%	71,74: 13.7%
73,75: 12.3%	77,81: 11.1%	14,17: 11.0%	

Table 2. The target sites $R[i, j]$ of *sodB* (interacts with *RyhB*) whose probabilities larger than 10^{-1} .

87,93: 63.8%	39,48: 50.7%	62,64: 43.6%	70,72: 39.6%
30,30: 28.4%	70,73: 27.0%	39,45: 17.0%	87,92: 13.5%
40,45: 11.9%	63,64: 11.4%		

Table 3. The target sites $R[i, j]$ of *fhlA* (interacts with *OxyS*) whose probabilities larger than 10^{-1} .

the key observation is that sampling probability for a case is equivalent to the contribution to partition function by the case divided by the partition function. For instance, again we consider the decomposition of $J_{i,j;h,\ell}^{RT, MK}$. Set \mathbb{P}_{i_1, j_1}^0 , \mathbb{P}_{i_1, j_1}^1 , \mathbb{P}_{i_1, j_1}^2 , \mathbb{P}_{i_1, j_1}^3 and \mathbb{P}_{i_1, j_1}^4 be the sampling probabilities for all five cases showed in Figure 8 (I) anticlockwise respectively, then we have:

$$\begin{aligned} \mathbb{P}_{i_1, j_1}^0 &= Q_{i_1, i_1; h_1, h_1}^{Hy, KK} Q_{i_1+1, j_1; h_1+1, \ell}^{RT, KKA} / Q_{i_1, j_1; h_1, \ell}^{RT, MK}, \\ \mathbb{P}_{i_1, j_1}^1 &= Q_{i_1, i_1; h_1, h_1}^{Hy, KK} Q_{i_1+1, j_1; h_1+1, \ell}^{RT, KF} / Q_{i_1, j_1; h_1, \ell}^{RT, MK}, \\ \mathbb{P}_{i_1, j_1}^2 &= Q_{i_1, i_1; h_1, h_1}^{Hy, KK} Q_{i_1+1, j_1; h_1+1, \ell}^{RT, FF} / Q_{i_1, j_1; h_1, \ell}^{RT, MK}, \\ \mathbb{P}_{i_1, j_1}^3 &= Q_{i_1, i_1; h_1, h_1}^{Hy, KK} Q_{i_1+1, j_1; h_1+1, \ell}^{RT, FK} / Q_{i_1, j_1; h_1, \ell}^{RT, MK}, \\ \mathbb{P}_{i_1, j_1}^4 &= Q_{i_1, j_1; h_1, \ell}^{Hy, KK} / Q_{i_1, j_1; h_1, \ell}^{RT, MK}. \end{aligned}$$

Since the probabilities of all mutually exclusive and exhaustive cases sum up to 1, we have $\sum_{i_1, j_1} \mathbb{P}_{i_1, j_1}^0 + \mathbb{P}_{i_1, j_1}^1 + \mathbb{P}_{i_1, j_1}^2 + \mathbb{P}_{i_1, j_1}^3 + \mathbb{P}_{i_1, j_1}^4 = 1$, which coincides with eqn. (2.1).

Next we give a description of the sampling algorithm, as a generalization of Ding and Lawrence (2003), we still take two stacks A and B . Stack A stores sub-joint structures and their types ξ in the form of $\{(i, j; h, \ell; \xi)\}$, such as $(i, j; h, \ell; RTMK)$ represents a sub-joint structure $J_{i,j;h,\ell}^{RT, MK}$. Stack B collects interior/exterior arcs and unpaired bases that will define a sampled interaction structure once the sampling process finishes. At the beginning, $(1, N; 1, M; \text{arbitrary})$ is the only element in stack A . A sampled interaction structure is drawn recursively as follows: at first, start with $(1, N; 1, M; \text{arbitrary})$, sample a pair of separated secondary structures or a rts $(i, N; j, M; RT\text{EE})$ according to their sampling probabilities. In the former case, $(1, N; j; \text{sec})$ and $(1, M; \text{sec})$ are stored in stack A . Otherwise, $(1, i-1; \text{sec})$, $(1, j-1; \text{sec})$ and $(i, N; j, M; RT\text{EE})$ are stored in stack A . Secondly, given a new element in stack A , denoted by $\{(i, j; h, \ell; \xi)\}$, we draw a particular case from all the mutual exclusive and exhaustive cases according to the sampling probabilities and store the corresponding sub-joint structures into stack A , and all the interior arc, exterior arc or unpaired bases sampled in the process will be stored in stack B . I.e. after the completion of sampling for a “bigger” joint structure from stack A and storage of “smaller” sub-joint structures derived in the former process in stack A , also the storage of the sampled arcs and unpaired bases of stack B , the element in

the bottom of stack A is chosen to do the subsequent sampling. The who process terminates when stack A is empty and at the same time, a sampled interaction structure formed in stack B .

4 RESULTS AND CONCLUSIONS

The complete set of recursions comprises for $ts\ Q_{i,j;r,s}^{\Delta,\nabla,\square}$, 15 4D-arrays respectively, for right-tight structures $Q_{i,j;r,s}^{RT}$, 20 4D-arrays, for dts $Q_{i,j;r,s}^{DT}$ and 20 4D-arrays. In addition, we need the usual matrices for the secondary structures R and S , and the above mentioned matrices for kissing loops. The full set of recursions is compiled in the SM, Section 3.

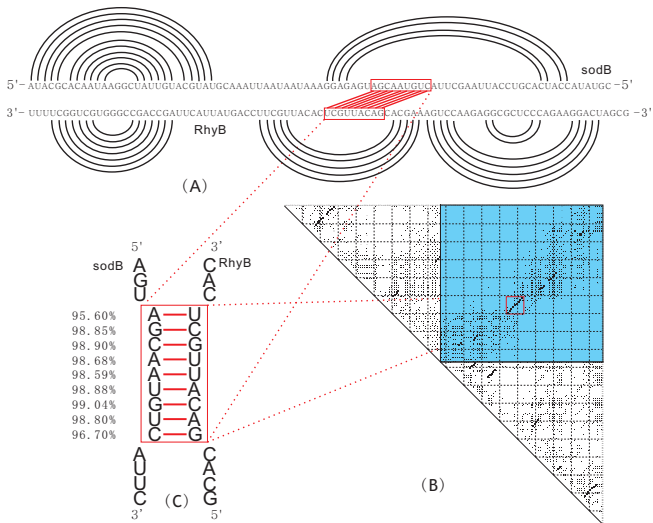


Fig. 9. (A) The natural structure of *sodB-RhyB* (Geissmann and Touati, 2004). (B) The hybrid-probability matrix generated via *rip2.0*. This matrix represents all potential contact regions of the *sodB* structure as squares, whose area is proportional to their respective probability. (C) “Zoom” into the most likely interaction region as predicted by *rip2.0*. All base pairs of the hybrid are labeled by their probabilities.

ACKNOWLEDGEMENTS

We thank Bill Chen and Sven Findeiß for comments on the manuscript. This work was supported by the 973 Project of the Ministry of Science and Technology, the PCSIRT Project of the Ministry of Education, and the National Science Foundation of China to CMR and his lab, grant No. STA 850/7-1 of the Deutsche Forschungsgemeinschaft under the auspices of SPP-1258 “Small Regulatory RNAs in Prokaryotes”, as well as the European Community FP-6 project SYNLET (Contract Number 043312) to PFS and his lab.

REFERENCES

Akutsu, T. (2000) Dynamic programming algorithms for RNA secondary structure prediction with pseudoknots. *Disc. Appl. Math.*, **104**, 45–62.
 Alkan, C., Karakoc, E., Nadeau, J., Sahinalp, S. and Zhang, K. (2006) RNA-RNA interaction prediction and antisense RNA target search. *J. Comput. Biol.*, **13**, 267–282.

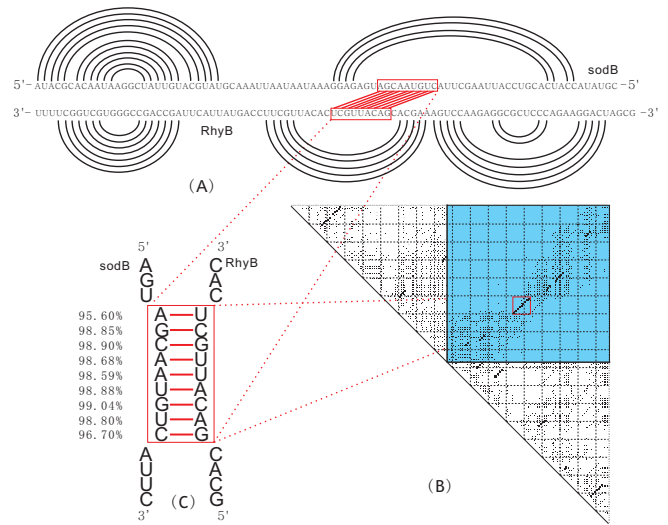
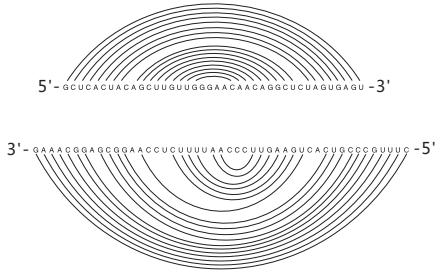
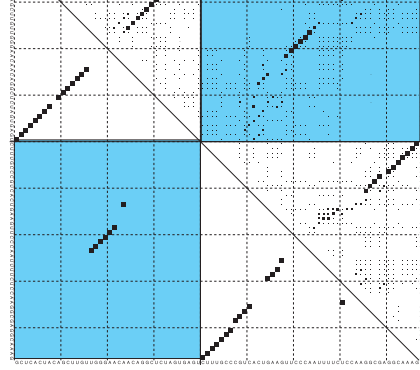
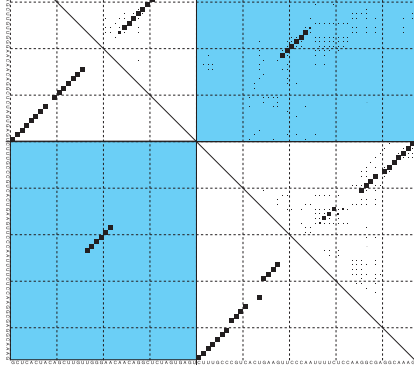
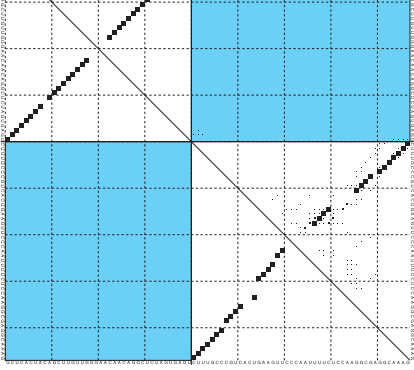


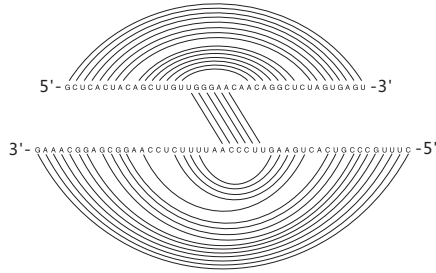
Fig. 10. (A) The natural structure of *sodB-RhyB* (Geissmann and Touati, 2004). (B) The hybrid-probability matrix generated via *rip2.0*. This matrix represents all potential contact regions of the *sodB* structure as squares, whose area is proportional to their respective probability. (C) “Zoom” into the most likely interaction region as predicted by *rip2.0*. All base pairs of the hybrid are labeled by their probabilities.

Ameres, S. and Schroeder, R. (2007) Molecular basis for target RNA recognition and cleavage by human RISC. *Cell*, **130**, 101–112.
 Andronescu, M., Zhang, Z. and Condon, A. (2005) Secondary structure prediction of interacting RNA molecules. *J. Mol. Biol.*, **345**, 1101–1112.
 Bachellerie, J., Cavallé, J. and Huttenhofer, A. (2002) The expanding snoRNA world. *Biochimie*, **84**, 775–790.
 Banerjee, D. and Slack, F. (2002) Control of developmental timing by small temporal RNAs: a paradigm for RNA-mediated regulation of gene expression. *Bioessays*, **24**, 119–129.
 Benne, R. (1992) RNA editing in trypanosomes. the use of guide RNAs. *Mol. Biol. Rep.*, **16**, 217–227.
 Bernhart, S., Tafer, H., Mückstein, U., Flamm, C., Stadler, P. and Hofacker, I. (2006) Partition function and base pairing probabilities of RNA heterodimers. *Algorithms Mol. Biol.*, **1**, 3–3.
 Busch, A., Richter, A. and Backofen, R. (2008) IntaRNA: efficient prediction of bacterial sRNA targets incorporating target site accessibility and seed regions. *Bioinformatics*, **24**, 2849–2856.
 Chitsaz, H., Salari, R., Sahinalp, S. and Backofen, R. (2009) A partition function algorithm for interacting nucleic acid strands. In press.
 Ding, Y. and Lawrence, C. (2003) A statistical sampling algorithm for rna secondary structure prediction. *Nucleic Acid Res.*, **31**, 7280–7301.
 Geissmann, T. and Touati, D. (2004) Hfq, a new chaperoning role: binding to messenger RNA determines access for small RNA regulator. *EMBO J.*, **23**, 396–405.
 Giegerich, R. and Meyer, C. (2002) *Lecture Notes In Computer Science*, volume 2422, chapter Algebraic Dynamic Programming, pp. 349–364. Springer-Verlag.
 Hofacker, I., Fontana, W., Stadler, P., Bonhoeffer, L., Tacker, M. and Schuster, P. (1994) Fast folding and comparison of RNA secondary structures. *Monatsh. Chem.*, **125**, 167–188.
 Huang, F., Qin, J., Stadler, P. and Reidys, C. (2009) Partition function and base pairing probabilities for RNA-RNA interaction prediction. *Bioinformatics*.
 Kertesz, M., Iovino, N., Unnerstall, U., Gaul, U. and Segal, E. (2007) The role of site accessibility in microRNA target recognition. *Nat. Genet.*, **39**, 1278–1284.
 Kretschmer-Kazemi Far, R. and Sczakiel, G. (2003) The activity of siRNA in mammalian cells is related to structural target accessibility: a comparison with antisense oligonucleotides. *Nucleic Acid Res.*, **31**, 4417–4424.
 Kugel, J. and Goodrich, J. (2007) An RNA transcriptional regulator templates its own regulatory RNA. *Nat. Struct. Mol. Biol.*, **3**, 89–90.

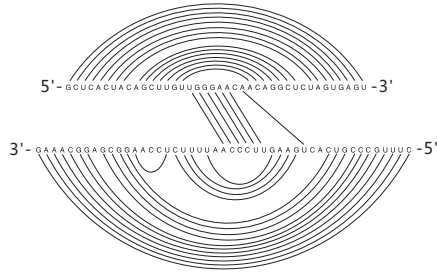
- McCaskill, J. (1990) The equilibrium partition function and base pair binding probabilities for RNA secondary structure. *Biopolymers*, **29**, 1105–1119.
- McManus, M. and Sharp, P. (2002) Gene silencing in mammals by small interfering RNAs. *Nature Reviews*, **3**, 737–747.
- Mneimneh, S. (2007) On the approximation of optimal structures for RNA-RNA interaction. *IEEE/ACM Trans. Comp. Biol. Bioinf.* In press, doi.ieeecomputersociety.org/10.1109/TCBB.2007.70258.
- Mückstein, U., Tafer, H., Bernhard, S., Hernandez-Rosales, M., Vogel, J., Stadler, P. and Hofacker, I. (2008) Translational control by RNA-RNA interaction: Improved computation of RNA-RNA binding thermodynamics. In Elloumi, M., Küng, J., Linial, M., Murphy, R. F., Schneider, K. and Toma, C. T. (eds.), *Bioinformatics Research and Development — BIRD 2008*, volume 13 of *Comm. Comp. Inf. Sci.*, pp. 114–127. Springer, Berlin.
- Mückstein, U., Tafer, H., Hackermüller, J., Bernhard, S., Stadler, P. and Hofacker, I. (2006) Thermodynamics of RNA-RNA binding. *Bioinformatics*, **22**, 1177–1182. Earlier version in: *German Conference on Bioinformatics 2005*, Torda Andrew and Kurtz, Stefan and Rarey, Matthias (eds.), *Lecture Notes in Informatics P-71*, pp 3-13, Gesellschaft f. Informatik, Bonn 2005.
- Narberhaus, F. and Vogel, J. (2007) Sensory and regulatory RNAs in prokaryotes: A new german research focus. *RNA Biol.*, **4**, 160–164.
- Pervouchine, D. (2004) IRIS: Intermolecular RNA interaction search. *Proc. Genome Informatics*, **15**, 92–101.
- Qin, J. and Reidys, C. (2008) A framework for RNA tertiary interaction. Submitted.
- Rehmsmeier, M., Steffen, P., Höchsmann, M. and Giegerich, R. (2004) Fast and effective prediction of microRNA/target duplexes. *Gene*, **10**, 1507–1517.
- Ren, J., Rastegari, B., Condon, A. and Hoos, H. (2005) Hotknots: heuristic prediction of microRNA secondary structures including pseudoknots. *RNA*, **11**, 1494–1504.
- Rivas, E. and Eddy, S. (1999) A dynamic programming algorithms for RNA structure prediction including pseudoknots. *J. Mol. Biol.*, **285**, 2053–2068.
- Storz, G. (2002) An expanding universe of noncoding RNAs. *Science*, **296**, 140–144.
- Tafer, H., Kehr, S., Hertel, J. and Stadler, P. (2009) RNAsnoop: Efficient target prediction for box H/ACA snoRNAs. Submitted.
- Tjaden, B., Goodwin, S., Opdyke, J., Guillier, M., Fu, D., Gottesman, S. and Storz, G. (2006) Target prediction for small, noncoding RNAs in bacteria. *Nucleic Acids Res.*, **34**, 2791–2802.
- Udekwi, K., Darfeuille, F., Vogel, J., Reimegård, J., Holmqvist, E. and Wagner, E. (2005) Hfq-dependent regulation of OmpA synthesis is mediated by an antisense RNA. *Genes Dev.*, **19**, 2355–2366.



(A)



(B)



(C)